JOURNAL OF CATALYSIS 69, 254–273 (1981)

Sintering of Palladium on Alumina Model Catalyst in a Hydrogen Atmosphere

JAMES J. CHEN AND ELI RUCKENSTEIN[1]

Department of Chemical Engineering, State University of New York at Buffalo, Amherst, New York 14260

Received June 26, 1980; revised December 23, 1980

The sintering behavior of Pd crystallites supported on γ-alumina in 1 atm flowing hydrogen as a function of time and temperature is reported. Model catalysts consisting of Pd crystallites supported on thin films of alumina are heated at 650, 725, and 800°C for various time intervals. The same region of a specimen is examined with a transmission electron microscope after each heat treatment to follow the changes of each Pd crystallite. The various events which occur during short, intermediate, and long durations of heating, are identified. The possible mechanisms are outlined and discussed.

INTRODUCTION

The supported metal catalysts are widely used in petrochemical, chemical, and automotive industries. They consist of small metal crystallites dispersed on a support of high surface area such as alumina or silica. Sintering of metal particles which occurs at high temperature results in a decrease of the active metal surface area. This affects the activity and sometimes the selectivity of the catalyst.

Supported palladium catalysts are mainly used as petroleum-reforming catalysts and automotive exhaust catalysts. Substantial sintering of Pd supported on alumina during heating in hydrogen has been found (*1*, *2*). Just 1 hr of heating at 650°C was enough to decrease the dispersion by 60% (*1*). In contrast to Pt/Al_2O_3 catalysts (*3–9*), the sintering kinetics of Pd/Al_2O_3 catalysts have not been systematically studied.

The purpose of this paper is to obtain information about the behavior of Pd crystallites as a function of time and temperature. Model catalysts containing very small Pd particles dispersed on a thin alumina film were heated in hydrogen for various time intervals at 650, 725, and 800°C. Samples were examined in a JEOL 100U transmission electron microscope (TEM). The same region of a specimen was observed after each heat treatment to follow the change in size, shape, and position of each particle. About 1000 to 1500 crystallites were measured to obtain the size distribution. Numerous events have been examined at various stages of heating with the goal of identifying possible mechanisms by which sintering occurs. Crystallite migration and coalescence seem to play a role in the sintering process. Direct ripening which involves atomic migration between pairs or a few neighboring particles with the smaller particle decreasing in size and then disappearing also has been observed occasionally. The disappearance of a large number of small crystallites all over the surface could be explained either by crystallite migration and coalescence or by Ostwald ripening. In contrast to the local direct ripening, Ostwald ripening is a global process involving a large number of particles and a two-dimensional phase of single metal atoms on the substrate.

EXPERIMENTAL PROCEDURES

Preparation of Thin Alumina Films

A thin (0.025 mm) high-purity (99.999%) aluminum foil was first chemically cleaned

---

[1] Correspondence concerning this paper should be addressed to E. Ruckenstein.

0021-9517/81/060254-20$02.00/0

in a polishing solution of orthophosphoric acid and nitric acid and then anodized at 20 V for 30 sec in a 3%wt tartaric acid solution at a pH of 5.5. The details of the anodic oxidation procedure to prepare thin films of alumina have been described in previous papers of this laboratory (*9, 10*). The nonporous and amorphous oxide film thus built up on aluminum was about 300 Å thick. The alumina film was separated from the unoxidized portion by floating small squares of foil on a dilute mercuric chloride solution in which aluminum dissolved. The films were then washed in distilled water. Finally, they were picked up on gold microscope grids and dried in air. The samples were calcinated in air at 800°C for 72 hr to transform amorphous alumina into crystalline γ-alumina (confirmed by electron diffraction). This prolonged heat treatment ensured that no further phase transformation and no displacements of the grains of the substrate would occur during the sintering experiments.

Preparation of the Model Catalyst

A thin Pd film about 15 Å thick was vacuum evaporated on to the support in an Edwards 306 vacuum coater at pressure below 10^{-6} Torr. The support was kept at room temperature during deposition. Pd wire of 99.999% purity wound on tungsten filament was the source. The film thickness could be controlled by the amount of Pd and the distance between source and target. The Pd/Al_2O_3 samples were heated at 500°C in flowing hydrogen inside a quartz tube for 6 hr to produce small Pd crystallites. This initial size distribution had crystallite diameters in the range of 10 to 70 Å.

Heat Treatment

All the sintering experiments were carried out at 1 atm in a quartz tube 5 ft. long and 1.5 in. in diameter in a 2-ft. tubular furnace. The following procedures were adopted to reduce the time span of heating-up and cooling-down. The quartz tube was first evacuated to 10^{-2} Torr and then nitrogen was introduced to flow through. The middle section of the tube was heated up to the desired temperatures in about 2 to 4 hr. In the meantime, samples sitting in a ceramic boat and being placed into the tube before evacuation were staying at room temperature at the end of the tube where nitrogen was flowing in. The ceramic boat was then displaced by a stainless-steel rod to the middle of the tube where its temperature reached the desired temperature in 3 to 5 min. Then hydrogen, replacing nitrogen, started to flow into the tube. As soon as the prespecified time interval was reached, the furnace was turned off and the samples were cooled down in a nitrogen stream. Compressed laboratory air was allowed to flow through the annular region between furnace and tube such that the tube temperature dropped to 500°C in 1.5 to 2.5 min. Preliminary experiments showed that no sintering took place at 500°C. Then the air flow rate was reduced so that the system slowly cooled to room temperature in about 1.5 hr to avoid the generation of strain in the crystallites. Nitrogen and hydrogen gases were provided by Linde Division, Union Carbide Corporation, and have a minimum purity of 99.999%. Before entering the tube, the gas passed through a column of 5A molecular sieves to remove any trace of water. The flow rate of the gases was 30 ml/min.

The same region of a specimen was examined after each heat treatment to follow the change in size, shape, and position of each particle. In each temperature series several regions of two or three similar specimens were examined. Heating effects due to electron bombardment in the microscope were largely eliminated by keeping the illumination intensity at about one-tenth of the level at which modifications in the samples were noticed. Samples were stored in a vacuum desiccator between each of the steps of the experiment to avoid contamination.

RESULTS

Figure 1 and Table 1 summarize various events observed during the sintering process on electron micrographs. It includes the disappearance of small crystallites, crystallite migration, crystallite migration and coalescence, the appearance of new crystallites, direct ripening, and faceting.

The size distribution of Pd crystallites at every stage was measured. In order for the size distribution to represent the whole population as closely as possible, the total number of crystallites examined at every stage was between 1000 and 1500. Two kinds of average sizes are reported here. They are defined as number-average diameter:

$$\bar{D}_n = \Sigma N_i\bar{D}_i/\Sigma N_i \qquad (1)$$

and surface-average diameter:

$$\bar{D}_s = \Sigma N_i\bar{D}_i^3/\Sigma N_i\bar{D}_i^2. \qquad (2)$$

By assuming hemispherical crystallites, the specific surface area, defined as the surface

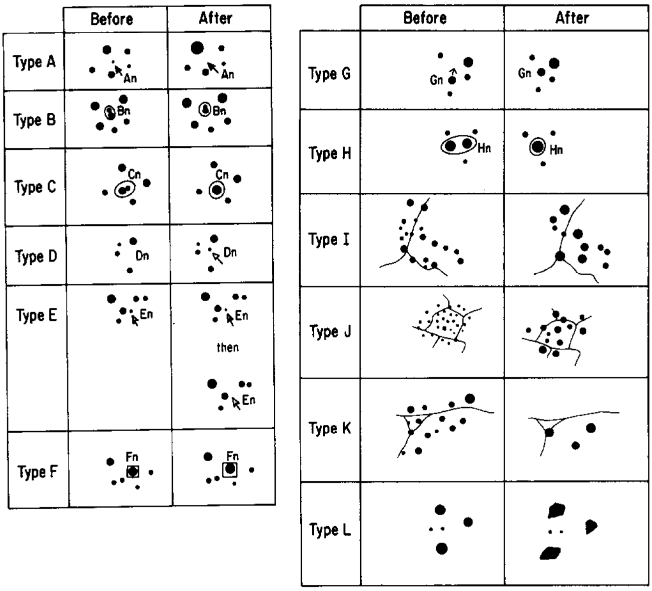

FIG. 1. Schematic illustration of various events observed during the sintering process: (Type A) Small crystallite disappears. Surrounding larger crystallites are stationary and either do not change or grow in size. (Type B) Two neighboring crystallites come in contact with each other and either do not change or grow in their sizes. (Type C) Two touching crystallites coalesce into a larger one. (Type D) A new crystallite appears at a place where no crystallite was located before. The previous location of this new crystallite is unknown. (Type E) A small crystallite very close to a larger one decreases in size and then disappears. (Type F) Crystallite is stationary and grows in size. (Type G) A crystallite migrates to a new position and grows or remains unchanged in size. (Type H) Two or more neighboring crystallites coalesce into a new crystallite somewhere between their original positions. (Type I) (The schemes I, J, and K contain grain boundaries. These events can, however, occur everywhere and not just near grain boundaries.) This is a global event which involves many crystallites. The former situation occurs after 30 min of heating at 650°C. The latter situation occurs after an additional 30 min of heating at the same temperature. The process leads to a new distribution of crystallites with larger diameters. (Type J) This event occurs during the first 10 min of heating of fresh catalyst at 725 and 800°C. The process is similar to a Type I event. (Type K) This event occurs during the additional 20 min of heating at 725°C after the first 10 min. The process is similar to that of a Type I event. (Type L) The shape of large crystallites, with diameter of about 125 Å or beyond, changes from spherical to faceted while those of the small ones remain unchanged.

TABLE 1

Possible Mechanisms and Examples of the Events of Fig. 1 Observed on the Electron Micrographs

Type	Possible mechanisms	Examples
A	There are two possible mechanisms. In the first, the small crystallite migrates and coalesces with one of the large ones. In the second, the small crystallite emits single atoms onto the substrate surface and either disappears or becomes smaller than the resolution of the electron microscope. The large crystallites capture the emitted single atoms.	A_1 to A_5 of Figs. 2a (before) and b (after); A_6 to A_{10} of Figs. 2b (before) and c (after); A_{11} to A_{13} of Figs. 2d (before) and e (after).
B	The process implies some displacement of particles.	B_1 to B_4 of Figs. 2a (before) and b (after).
C	Crystallite coalescence.	C_1 of Figs. 2a (before) and b (after).
D	The migration and coalescence of very small particles with sizes below the resolution of the electron microscope (unresolved particles) is one of the possible mechanisms. The new crystallite could also form through direct ripening of the unresolved particles.	D_1 and D_2 of Figs. 2a (before) and b (after); D_3 to D_7 of Figs. 2d (before) and e (after).
E	The small crystallite transfers single atoms directly to the larger one. This phenomenon is called direct ripening and will be discussed in detail later.	E_1 and E_2 of Figs. 2a (before), b, and c (after); E_3 of Figs. 2d (before), e, and f (after).
F	The migration of unresolved particles and coalescence with the large one is one of the possible mechanisms. The unresolved particles could also be captured by the large one through direct ripening. Spreading of crystallites is also a possible mechanism.	F_1 and F_2 of Figs. 2b (before) and c (after).
G	The growth of the moving crystallite could possibly be attributed to its capture of small unresolved particles on the way to its new position.	G_1 to G_5 of Figs. 2d (before) and e (after).
H	This process may involve the migration and coalescence of crystallites and/or direct ripening.	H_1 to H_5 of Figs. 2d (before) and e (after); H_6 to H_8 of Figs. 2e (before) and f (after).
I	Because of the appearance of crystallites at places where no crystallites were located before, it seems that crystallite migration and coalescence are at least in part responsible for this process.	Figs. 2c (before) and d (after).
J	Similar to a Type I event.	Figs. 5a (before) and b (after).
K	Similar to a Type I event.	Figs. 5b (before) and c (after).
L	Faceting which occurs after extended heating on sufficiently large crystallites because this shape is thermodynamically more stable.	Figs. 5d (before) and e (after); Figs. 7a (before) and b (after).

area per gram of metal, is given by[2]

$$S = \left(\frac{\pi}{2}\right)(\Sigma\, N_i\bar{D}_i^2) \Big/ \left(\frac{\rho\pi}{12}\right)(\Sigma\, N_i\bar{D}_i^3) = 6/\rho\bar{D}_s, \quad (3)$$

where N_i is the number of crystallites with diameter between $\bar{D}_i - \Delta D_i/2$ and $\bar{D}_i + \Delta D_i/2$, $\bar{D}_i$ is the average diameter in each diameter interval, and ρ is the density of Pd.

Effect of Time and Temperature

Figures 2a–f show the time sequence of the same region heated at 650°C. As time progressed, the population density of crystallites decreased and the size of crystallites increased. For the first 30 min (Figs. 2a–c) all the changes occurred locally and the events which took place are of Types A to F of Fig. 1 and Table 1. The most drastic changes occurred between the third and the fourth stages (Figs. 2c and d), from $t = 30$ min to $t = 1$ hr. The event of Type I of Fig. 1 and Table 1 is the best description of these changes. Almost all the crystallites were involved in the process. The result was a new distribution of the crystallites. For comparison, the upper right part of Fig. 2c is overlapped in Fig. 3 over the corresponding part of Fig. 2d. The particles marked by solid lines and those marked by broken lines indicate the positions of the crystallites at the third and the fourth stages, respectively. Crystallite 2 probably originated from crystallite 1 which seems to migrate about 80 Å and to grow from 60 to 85 Å in diameter. Its growth in size probably took place either by the capturing of small particles with sizes below the resolution of the electron microscope and/or by spreading. Crystallite 5 might be the combination of crystallites 3 and 4. Crystallite 6 could have moved toward crystallite 7 to form crystallite 8. Crystallite 10 may have originated from crystallite 9 and the small crystallites (including some unresolved ones) nearby. Crystallite 13 probably formed by the migration of crystallite 11 across the grain boundary and the coalescence with crystallite 12. Similarly, migration and coalescence of crystallites 14 and 15 could have occurred and led to the formation of crystallite 16.

Since so many new crystallites appear in Fig. 2d at places where no crystallites have been located before (Fig. 2c) and the disappearance of crystallites in Fig. 2c suggest that a large-scale crystallite migration and coalescence might have occurred during this 30-min interval. An alternative explanation is atomic migration associated with nucleation of new particles at some sites where the interactions between metal particles and substrate are strong. Figure 3 seems to suggest that the latter explanation is less likely.

The sintering rate slowed down with further heating. All the events involved at most a few neighboring crystallites. Type G and H events of Fig. 1 and Table 1 seemed to dominate the latter stages of the process. Crystallites as large as 60 to 75 Å in diameter (events G_1 to G_5 of Figs. 2d and e) were observed to migrate. Events H_1 to H_5 of Figs. 2d and e involved two to five crystallites which coalesced into new crystallites. The appearance of new small crystallites without any evidence about their previous locations, events of Type D, indicates that some small crystallites might be generated through the coalescence or direct ripening of smaller particles and not necessarily through the decrease in size of crystallites.

Table 2 lists the events observed on the electron micrographs of all the regions examined after each treatment. Events B and C were found only during the early stages because they involve small crystallites and take place in a short time interval. Probably a Type H event replaced them during the latter stages.

---

[2] The actual shape of the crystallites is not hemispherical. Tilting experiments can provide information about the thickness of the crystallites. However, tilting capabilities are not available in this laboratory.

FIG. 2. Time sequence of the same region of Pd/Al_2O_3 model catalyst: (a) fresh catalyst; heated in 1 atm H_2 at 650°C for (b) 10 min; (c) 30 min; (d) 1 hr; (e) 4 hr; (f) 8 hr.

FIG. 2—*Continued.*

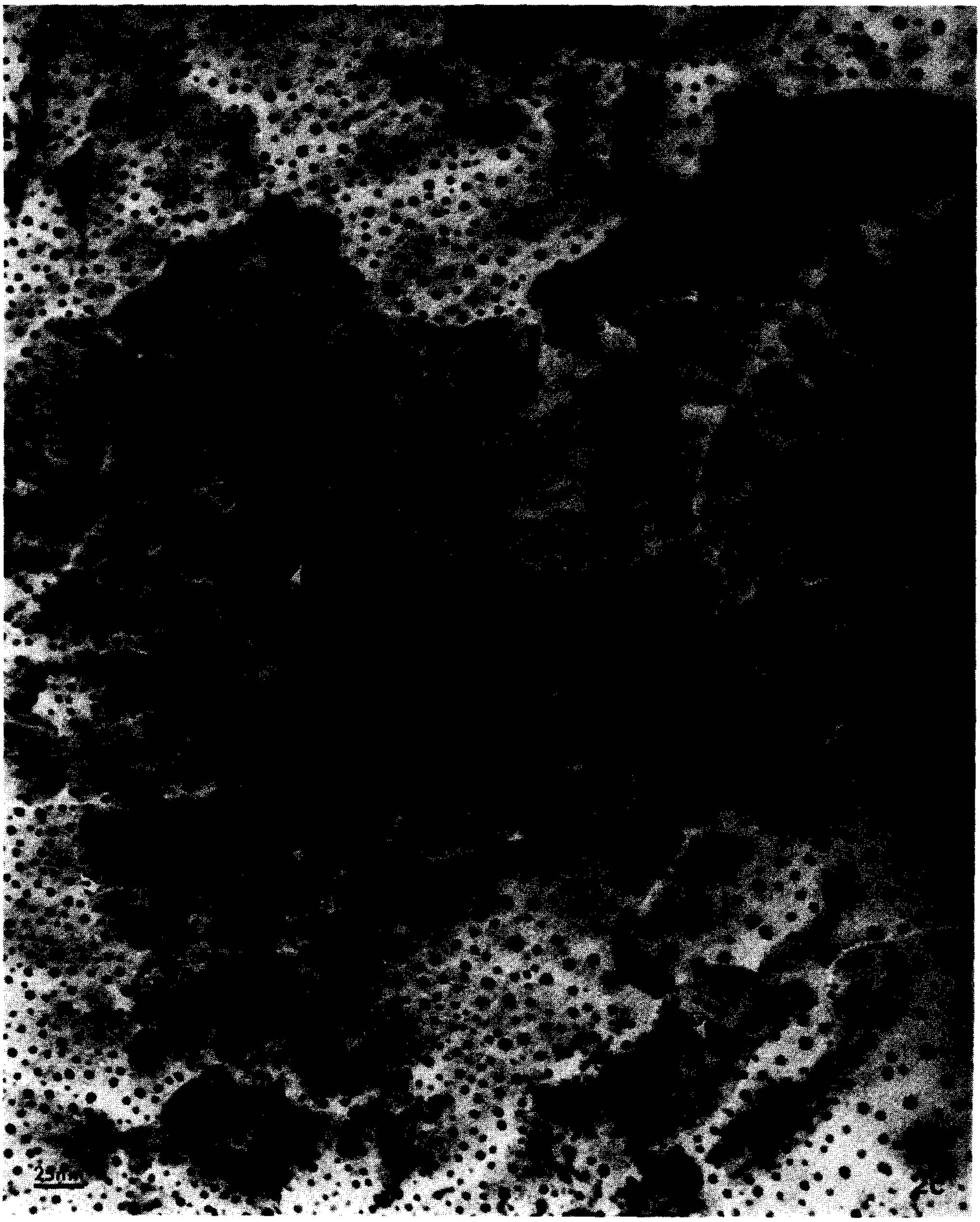

FIG. 2.—*Continued.*

FIG. 2.—*Continued.*

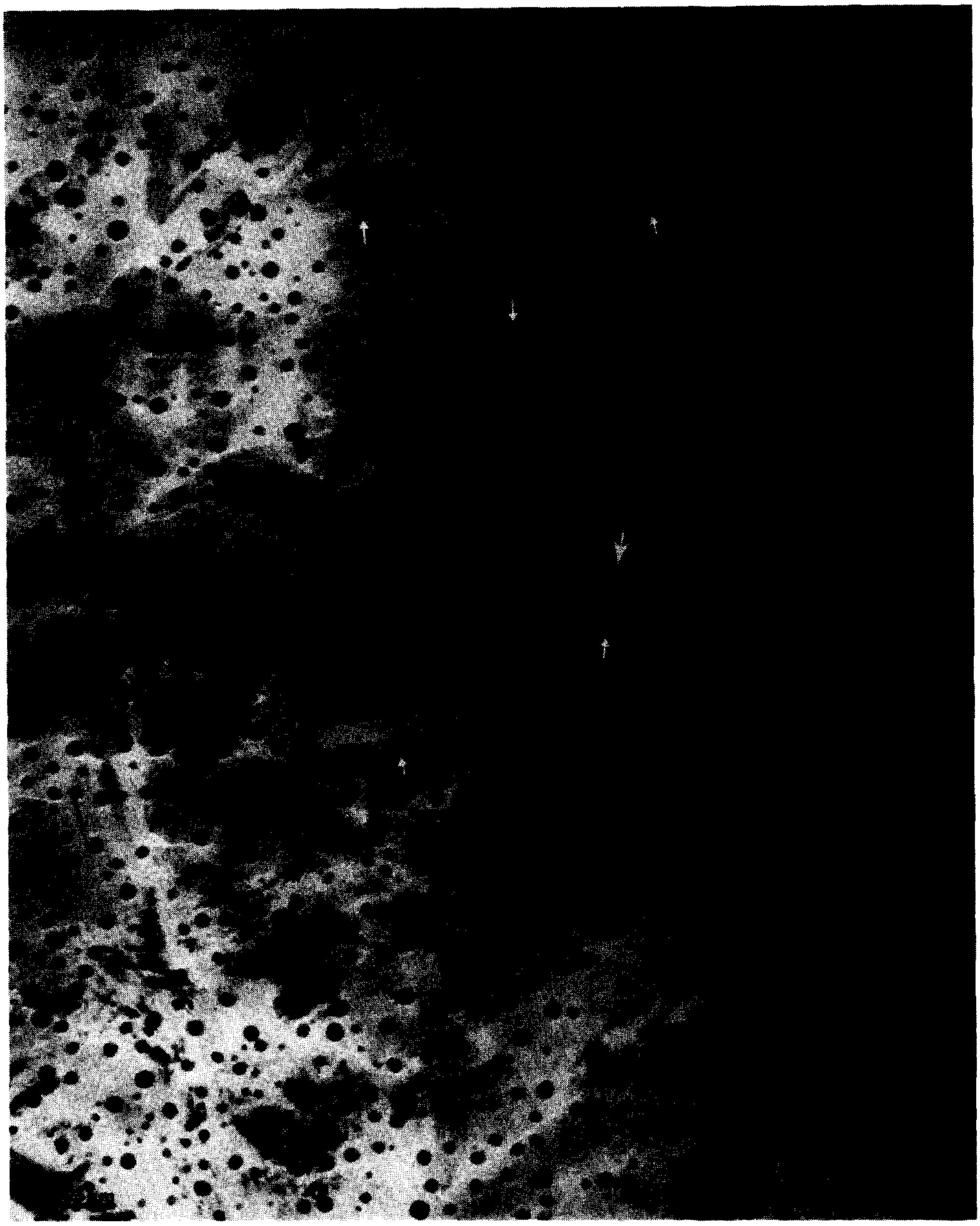

FIG. 2.—*Continued.*

FIG. 2.—*Continued.*

FIG. 3. Position distribution of the crystallites from Fig. 2c, solid lines, and Fig. 2d, broken lines.

Figures 4a–d give the size distribution of more than 1000 Pd crystallites at four different stages. As sintering proceeded, the percentage of small crystallites decreased, the curve broadened and developed tails toward the large-diameter side of the curve.

The time sequence of average crystallite size and surface area based on the size distribution is shown in Table 3. The drastic changes taking place between the third and the fourth stages are also reflected in the variation of the average diameter and surface area.

Figures 5a–e show the same region of the same specimen heated at 725°C for various lengths of time. It is impossible to follow the changes which occurred on each crystallite during the first 30 min, Figs. 5a–c, because the rate of sintering was extremely high. Types J and K events of Fig. 1 and Table 1 described the process. During further heating, the rate of sintering was much slower. Faceting of the crystallites larger than 125 Å in diameter occurred after 20 hr of heating (Fig. 5e).

Table 4 lists the events observed on all the regions examined. They are similar to the latter stages of the 650°C series. The size distributions shown in Figs. 6a–c are similar in shape to those at 650°C. However, a multimodal distribution starts to

TABLE 2

Events Observed during Sintering at 650°C

Time interval (hr)	Events
0–0.167	A^a, B, C, D, E^b, F
0.167–0.5	A^a, B, C, D, E^b, F
0.5–1	I
1–4	A, D, E^b, F, G, H^a
4–8	A, D, E^b, F^a, G, H
8–20	A, D^b, F^a, G, H

[a] Most frequently observed event.
[b] Least frequently observed event.

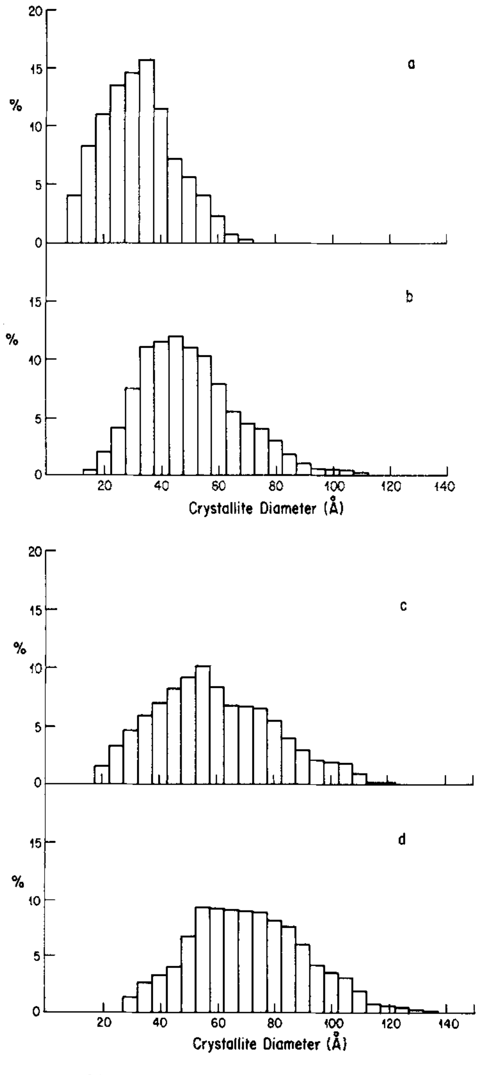

FIG. 4. Size distribution of Pd crystallites: (a) initial distribution; heated in 1 atm H_2 at 650°C for (b) 1 hr; (c) 4 hr; (d) 20 hr.

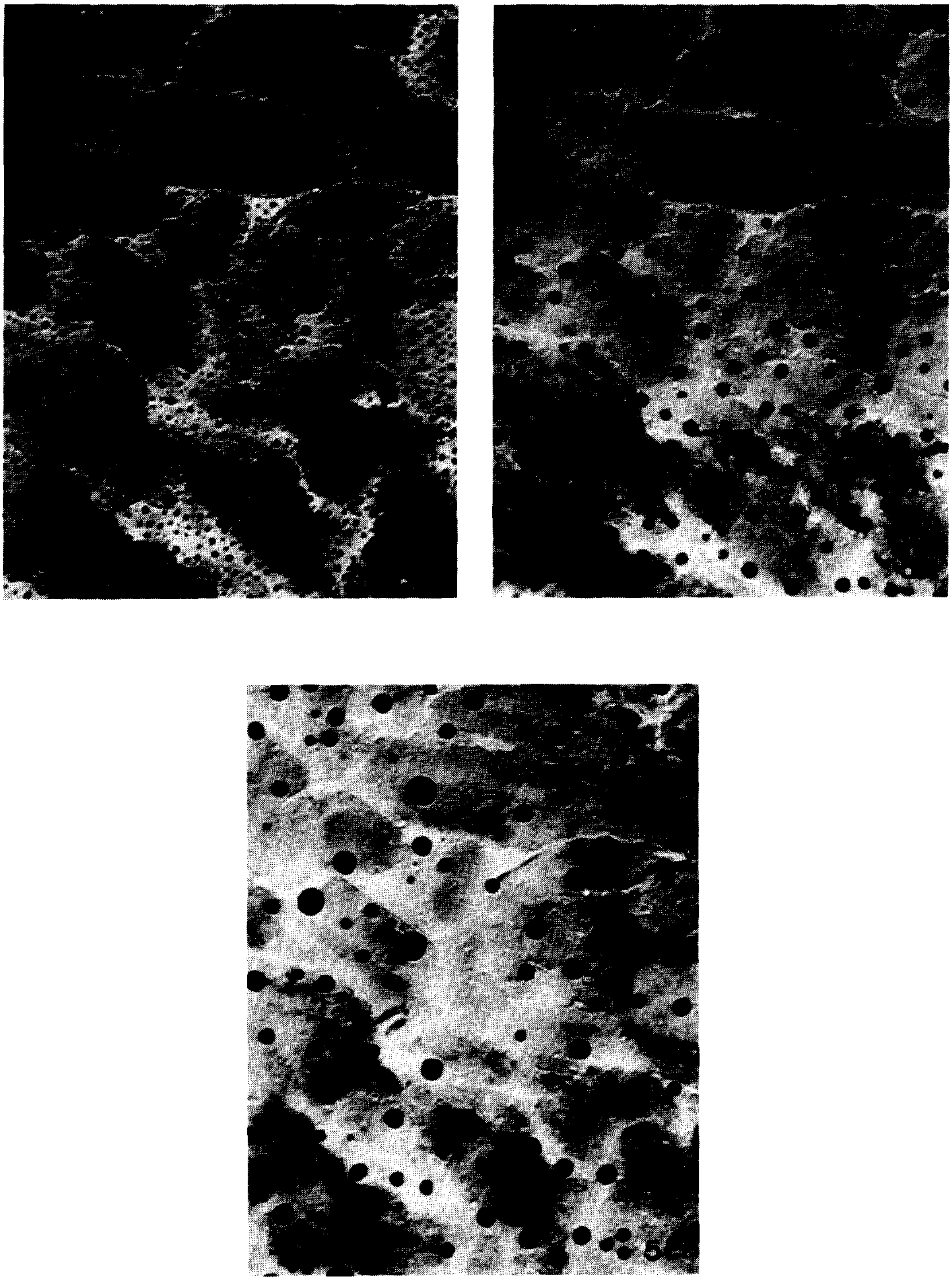

FIG. 5. Time sequence of the same region of Pd/Al_2O_3 model catalyst: (a) fresh catalyst; heated in 1 atm H_2 at 725°C for (b) 10 min; (c) 30 min; (d) 8 hr; (e) 20 hr.

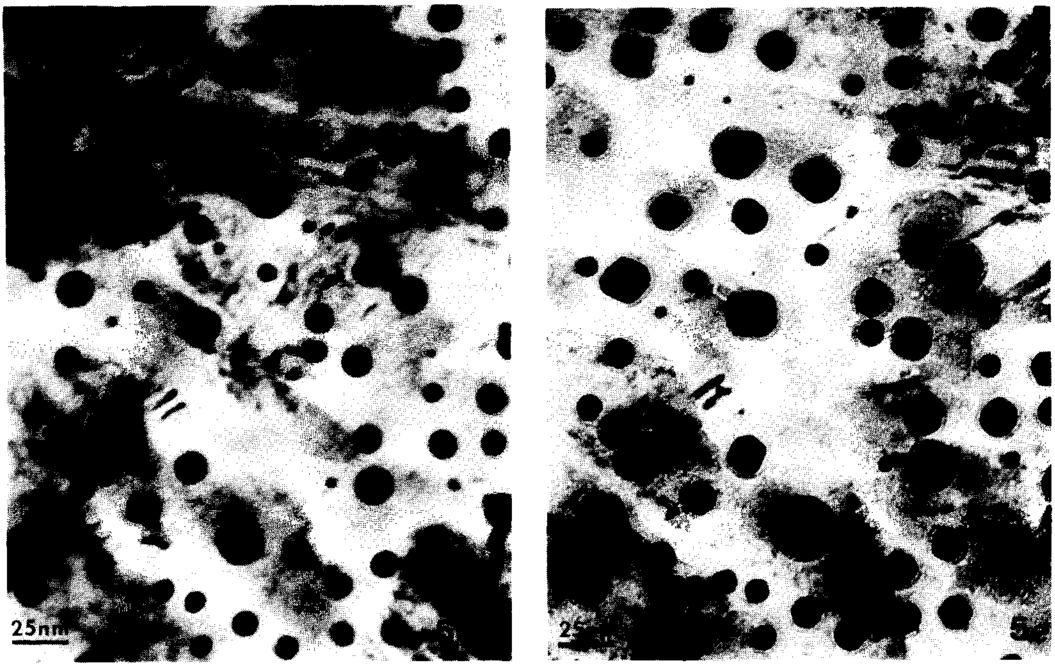

FIG. 5—*Continued.*

develop in Fig. 6d. This seems to be associated with the formation of faceted crystallites. The average crystallite size and surface area are listed in Table 5. The surface area dropped to 66% of the initial value during the first 10 min and reached 30% after 20 hr.

The events occurring during heating at 800°C are summarized in Table 6. (For average crystallite size and surface area see Table 7). In this case, a few faceted crystallites started to form just after 2 hr of treatment (Fig. 7a) and, almost all the large crystallites changed their shapes from spherical to faceted after 4 hr (Fig. 7b). At this stage, t = 4 hr, most crystallites had square, tetragonal, pentagonal, or hexagonal shape. Further sintering of these faceted crystallites led to the appearance of particles with more irregular shapes which show different contrast areas in a crystallite (Fig. 7c). Twinned crystallites might have

TABLE 3

Average Crystallite Size and Specific Surface Area of Pd/γ-Al_2O_3 at 650°C

Cumulative time (hr)	Number-average diameter (Å)	Surface-average diameter (Å)	Specific surface area (m^2/g Pd)	$\left(\frac{S}{S_0}\right)$
0	32.5	41.8	119.402	1.00
0.167 (10 min)	35.3	43.1	115.759	0.97
0.5	39.3	46.3	107.707	0.90
1	50.3	62.4	80.033	0.67
4	59.7	74.3	67.203	0.56
8	61.3	76.4	65.366	0.55
20	71.2	82.3	60.670	0.51

S: specific surface area at time t; S_0: initial specific surface area.

TABLE 4

Events Observed during Sintering at 725°C

Time interval (hr)	Events
0–0.167	J
0.167–0.5	K
0.5–1	A, D, E[a], F, G, H[b]
1–2	A, D, E[a], F, G, H[b]
2–4	A[a], D, F[b], G, H
4–8	A[a], D, F[b], G, H
8–20	A[a], D, F[b], G, H, L

[a] Least frequently observed event.
[b] Most frequently observed event.

formed (*11*) probably by the coalescence of neighboring crystallites.

The size distributions, Figs. 8a–d, started developing into a bimodal curve at $t = 4$ hr and became well-developed multimodal at $t = 20$ hr. The time at which the bimodal distribution appears seems to be related to the formation of faceted crystallites.

DISCUSSION

Two sintering mechanisms have been proposed. Ruckenstein and Pulvermacher (*12*, *13*) developed a scheme of migration and coalescence of metal crystallites over the support surface. Chakraverty (*14*) and Flynn and Wanke (*7*, *15*) have used the Ostwald ripening mechanism to account for sintering. In Ostwald ripening the large crystallites increase in size while the small ones decrease in size. Since these two mechanisms are not exclusive, a comprehensive treatment has been developed by Ruckenstein and Dadyburjor (*16*), which combines emission, migration, and coalescence of particles of every size, including single atoms.

Crystallite Migration

In Table 1 crystallite migration is listed as one of the possible mechanisms for various events. Crystallites as large as 75 Å in diameter were observed to migrate at 650°C (Figs. 2d and e). However, small crystallites such as X, Y, and Z of the same figures were found to remain stationary. This fact suggests that the mobility of the crystallites is not just a function of their size. Strictly speaking, the substrate surface is not homogeneous from a microscopic point of view. The local surface structure and the local surface irregularities affect the interaction force between crystallites and substrate. Therefore, the migration of crystallites on the surface of substrate may be a direction-selective process rather than a random walk-type diffusion process. Particular crystallites may migrate with preference in one direction but not in another. A small crystallite trapped in a valley will migrate with more difficulty than a larger

TABLE 5

Average Crystallite Size and Specific Surface Area of Pd/γ-Al_2O_3 at 725°C

Cumulative time (hr)	Number-average diameter (Å)	Surface-average diameter (Å)	Specific surface area (m^2/g Pd)	$\left(\frac{S}{S_0}\right)$
0	31.8	40.4	123.556	1.00
0.67 (10 min)	52.0	61.2	81.563	0.66
0.5	63.8	74.3	67.183	0.54
1	67.3	88.1	56.682	0.46
2	72.1	97.2	51.375	0.42
4	80.9	113.9	43.831	0.36
8	84.3	119.2	41.881	0.34
20	98.6	134.3	37.164	0.30

S: specific surface area at time t; S_0: initial specific surface area.

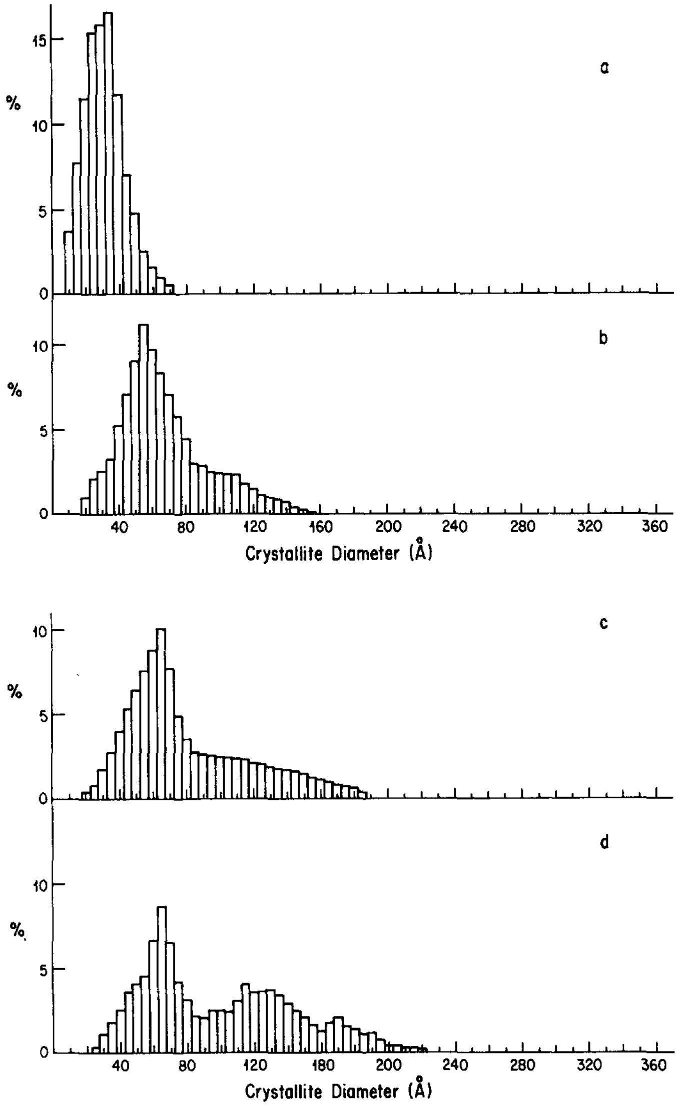

FIG. 6. Size distribution of Pd crystallites: (a) initial distribution; heated in 1 atm H_2 at 725°C for (b) 1 hr; (c) 4 hr; (d) 20 hr.

one which contacts only the tips of the hills of the surface.

Movements of the grain boundaries were not observed; nevertheless, local movements of the alumina substrate might have occurred, stimulating the migration of crystallites.

Ripening

Ripening is another possible mechanism for the sintering process. The equilibrium concentration of single atoms at the interface of a smaller particle is larger than that of a larger one. The equilibrium interface concentration of single atoms (expressed as atoms per unit area of substrate) for a particle of infinite size is the solubility of the system at that temperature. In a supersaturated system, i.e., a system in which the concentration of single atoms per unit area of substrate is greater than the solubility, the particles which have a radius

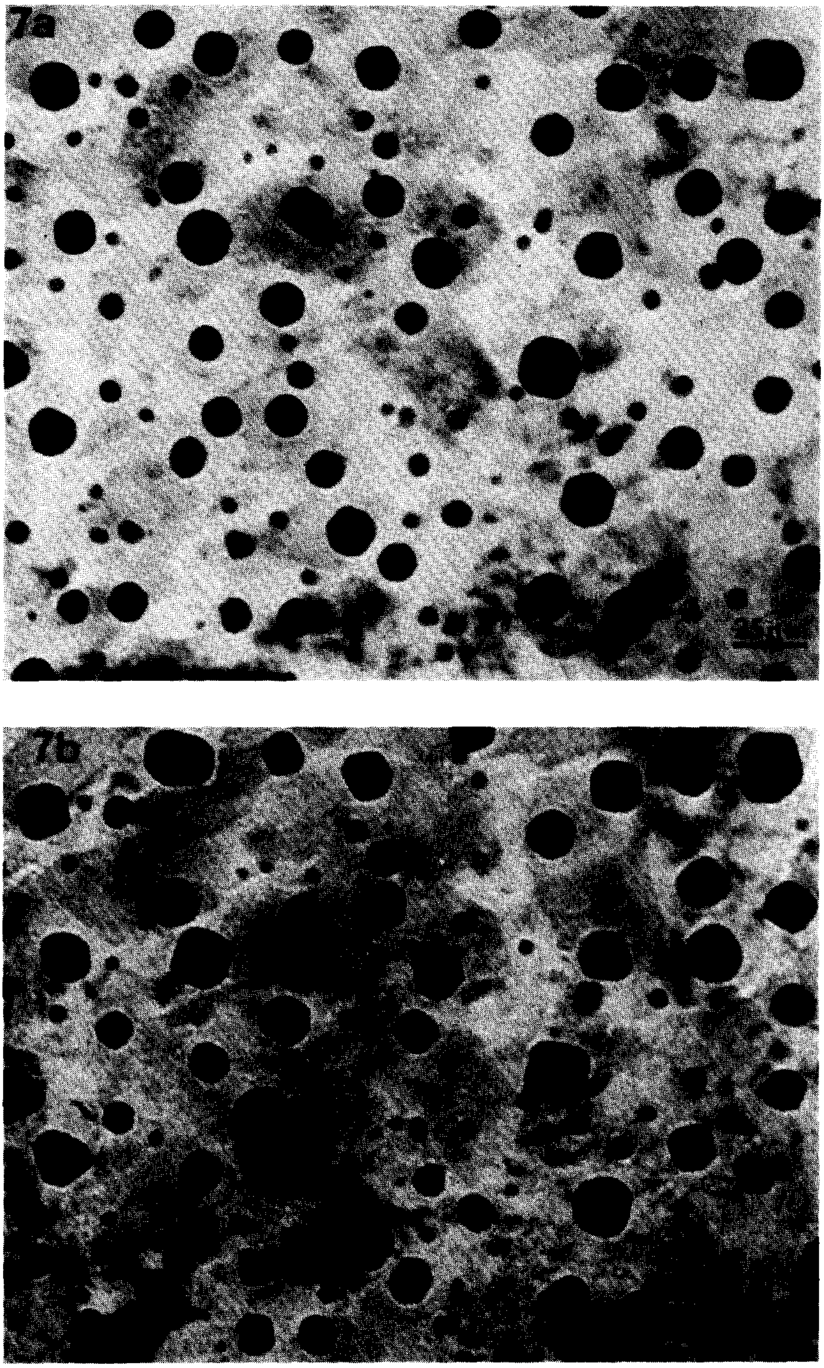

FIG. 7. Time sequence of the same region of Pd/Al_2O_3 model catalyst after heating in 1 atm H_2 at 800°C for (a) 2 hr; (b) 4 hr; (c) 20 hr.

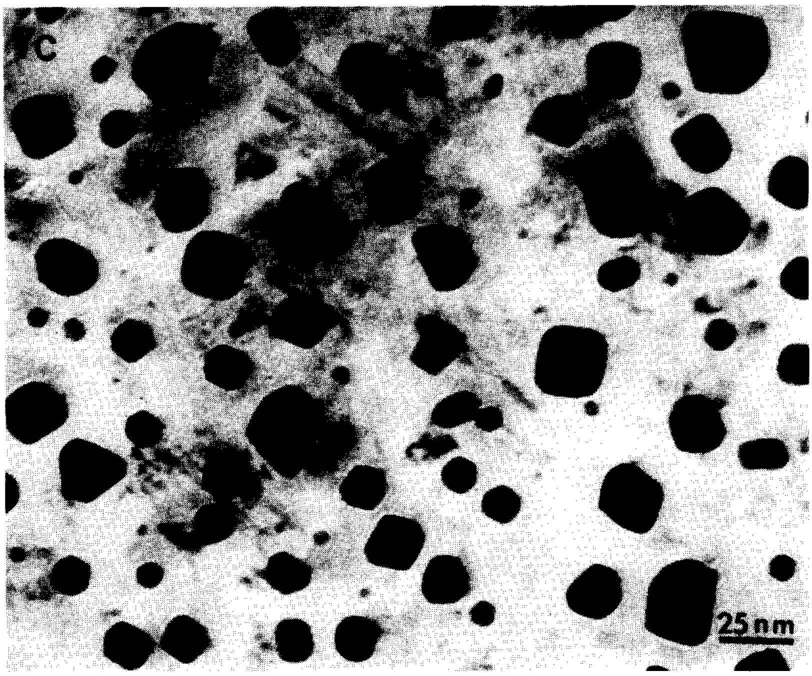

FIG. 7—*Continued.*

smaller than a critical value will release single atoms into the bulk and decrease in size. On the other hand, particles larger than the critical radius will gain single atoms from the bulk and increase in size. This occurs because for a supersaturated system, the equilibrium concentration at the leading edge of the smaller particles is larger than the bulk concentration, while that at the leading edge of the larger particles is smaller than the bulk concentration. The result is the growth of the larger particles at the expense of the smaller ones. This phenomenon is called Ostwald ripening and is a global process involving a two-dimensional phase of single atoms and a large number of particles. During the experiment, a large number of small crystallites were observed to disappear (Type A event) between consecutive stages, e.g., Figs. 2a (before) and b (after). Although there is no direct evidence to prove that they did first decrease in size and then disappear, the possibility of Ostwald ripening cannot be ruled out. Of course, the disappearance of these crystallites could also be explained via a migration–coalescence process.

A few small crystallites very close to a larger one were observed to decrease in size and then disappear (Type E event). This phenomenon which occurred in localized regions of the surface and involved only neighboring crystallites could possibly be explained by direct ripening (*17*). In contrast to Ostwald ripening which can

TABLE 6

Events Observed during Sintering at 800°C

Time interval (hr)	Events
0–0.167	J
0.167–0.5	A, D, E[a], F, G, H[b]
0.5–1	A, D, E[a], F, G, H[b]
1–2	A, D, F, G, H[b], L[a]
2–4	A[a], D, F[b], G, H, L
4–8	A, D, E[a], F, G, H[b]
8–20	A[a], D, F[b], G, H

[a] Least frequently observed event.
[b] Most frequently observed event.

TABLE 7

Average Crystallite Size and Specific Surface Area of Pd/γ-Al_2O_3 at 800°C

Cumulative time (hr)	Number-average diameter (Å)	Surface-average diameter (Å)	Specific surface area (m^2/g Pd)	$\left(\frac{S}{S_0}\right)$
0	31.7	41.0	121.748	1.00
0.167 (10 min.)	57.3	65.2	76.560	0.63
0.5	68.5	79.6	62.700	0.51
1	70.9	91.4	54.645	0.45
2	74.6	101.4	49.234	0.41
4	87.4	126.3	39.509	0.33
8	90.4	129.9	38.438	0.32
20	112.2	164.0	30.440	0.25

S: specific surface area at time *t*; S_0: initial specific surface area.

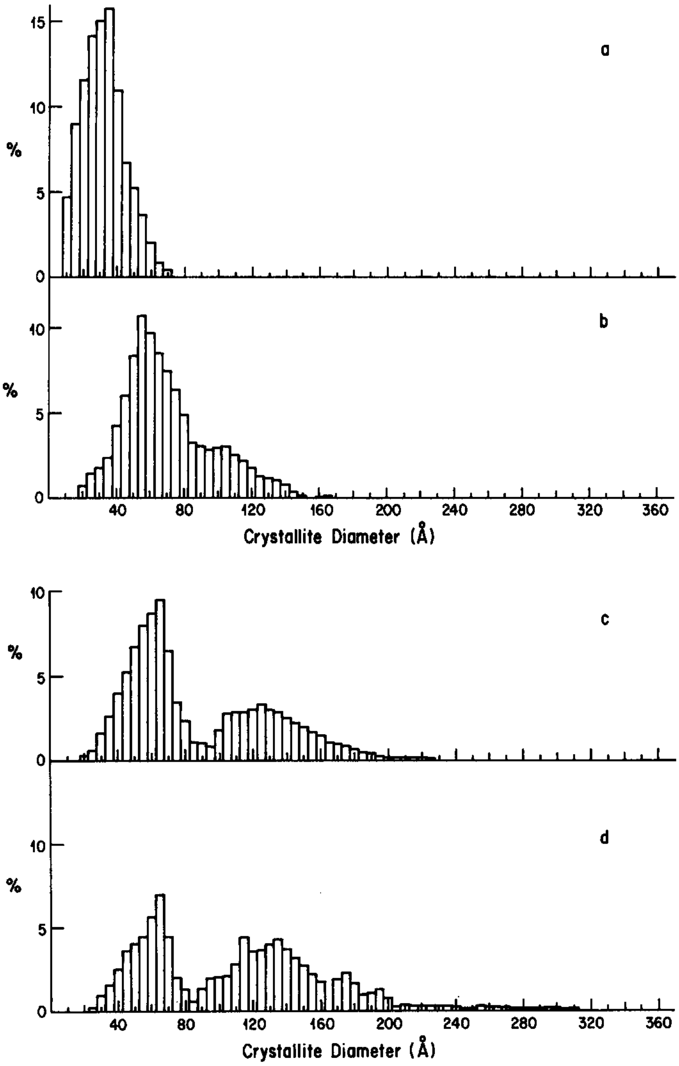

FIG. 8. Size distribution of Pd crystallites: (a) initial distribution; heated in 1 atm H_2 at 800°C for (b) 1 hr; (c) 4 hr; (d) 20 hr.

only occur in a supersaturated system, the direct ripening can occur even if the whole system is unsaturated. As long as two or more particles are close enough to one another, single atoms may transfer directly from the smaller to the larger one since the former has a higher surface pressure than the latter. It is a local event rather than a global process. The localized character of direct ripening probably stems from the heterogeneity of the (alumina) substrate surface, as well as from the particularities of the interactions at the leading edge of the crystallites.

CONCLUSION

The sintering of palladium on alumina during heating in a hydrogen atmosphere is a complex phenomenon which may occur via various mechanisms: (a) crystallite migration and coalescence; (b) direct ripening; and (c) Ostwald ripening. It seems that crystallite migration is not only dependent on the crystallite size and temperature but also on the irregularities of the substrate since the latter affect the interaction of crystallite with the substrate. In some cases, the location of the crystallite rather than its size affects the mobility. Evidence for direct ripening which involves atomic migration between a small and a larger particle is also brought. Ostwald ripening or migration and coalescence are two possible mechanisms which could explain the disappearance of a large number of small crystallites that was observed between two consecutive stages of heating.

REFERENCES

1. Klimisch, R. L., Summers, J. C., and Schlatter, J. C., *in* "Catalysts for the Control of Automotive Pollutants" (J. E. McEvoy, Ed.). Advances in Chemistry Series No. 143, Amer. Chem. Soc., Washington, D.C., 1975.
2. Aben, P. C., *J. Catal.* **10**, 224 (1968).
3. Herrmann, R., Adler, S. F., Goldstein, M. S., and DeBaun, R. M., *J. Phys. Chem.* **65**, 2189 (1961).
4. Graber, H. L., *J. Phys. Chem.* **66**, 48 (1962).
5. Somorjai, G., *Anal. Chem.* **1**, 101 (1968).
6. Maat, H. J., and Moscou, L., *in* "Proceedings, 3rd International Congress on Catalysis, Amsterdam, 1964," Vol. 11, p. 1277. Wiley, New York, 1965.
7. Flynn, P. C., and Wanke, S. E., *J. Catal.* **37**, 432 (1975).
8. Baker, R. T. K., Thomas, C., and Thomas, R. B., *J. Catal.* **38**, 510 (1975).
9. Chu, Y. F., and Ruckenstein, E., *J. Catal.* **55**, 281 (1978).
10. Ruckenstein, E., and Malhotra, M. L., *J. Catal.* **41**, 303 (1976).
11. Avery, N. R., and Sanders, J. V., *J. Catal.* **18**, 129 (1970).
12. Ruckenstein, E., and Pulvermacher, B., *AIChE J.* **19**, 356 (1973).
13. Ruckenstein, E., and Pulvermacher, B., *J. Catal.* **29**, 224 (1973).
14. Chakraverty, B. K., *J. Phys. Chem. Solids* **28**, 2401 (1967).
15. Flynn, P. C., and Wanke, S. E., *J. Catal.* **33**, 233 (1974).
16. Ruckenstein, E., and Dadyburjor, D., *J. Catal.* **48**, 73 (1977).
17. Ruckenstein, E., and Dadyburjor, D. B., *Thin Solid Films* **55**, 89 (1978).